University of Pennsylvania
ScholarlyCommons

Departmental Papers (MSE)

Department of Materials Science & Engineering

12-15-2005

Ionic Aggregates in Zn- and Na-neutralized Poly(ethylene-*ran*-methacrylic acid)

Nicholas M. Benetatos
University of Pennsylvania

Karen I. Winey
University of Pennsylvania, winey@lrsm.upenn.edu

Postprint version. "This is a preprint of an article published in *Journal of Polymer Science Part B - Polymer Physics*, Volume 43, Issue 24, December 15, 2005, pages 3549-3554."
Publisher URL: http://dx.doi.org/10.1002/polb.20623

This paper is posted at ScholarlyCommons. http://repository.upenn.edu/mse_papers/82
For more information, please contact repository@pobox.upenn.edu.

Ionic Aggregates in Zn- and Na-neutralized Poly(ethylene-*ran*-methacrylic acid)

Abstract
The morphology of ionic aggregates in semi-crystalline Zn- and Na-neutralized poly(ethylene-*ran*-methacrylic acid) (EMAA) ionomer blown films has been explored with scanning transmission electron microscopy (STEM) and small angle x-ray scattering (SAXS). The ionic aggregates of Zn-EMAA are spherical, monodisperse and uniformly-distributed in as-extruded pellets and blown films prepared at low and high blow-up ratio. Thus, although the biaxial stresses of film blowing are sufficient to alter the PE superstructure, the ionic aggregates in Zn-EMAA are unaffected. In contrast, the morphology of Na-EMAA as detected by STEM changes from featureless in the as-extruded pellets to a heterogeneous distribution of Na-rich aggregates in the blown films. This transformation in Na-EMAA morphology is consistent with our earlier study of quiescent annealing suggesting that the morphological change is the result of thermal processing rather than the biaxial stresses of film blowing.

Comments
Postprint version. "This is a preprint of an article published in *Journal of Polymer Science Part B - Polymer Physics*, Volume 43, Issue 24, December 15, 2005, pages 3549-3554."
Publisher URL: http://dx.doi.org/10.1002/polb.20623

This journal article is available at ScholarlyCommons: http://repository.upenn.edu/mse_papers/82

Ionic Aggregates in Zn- and Na-neutralized Poly(ethylene-*ran*-methacrylic acid) Blown Films

Nicholas M. Benetatos and Karen I. Winey*

Department of Materials Science and Engineering, University of Pennsylvania, Philadelphia, Pennsylvania 19104-6272

Abstract

The morphology of ionic aggregates in semi-crystalline Zn- and Na-neutralized poly(ethylene-*ran*-methacrylic acid) (EMAA) ionomer blown films has been explored with scanning transmission electron microscopy (STEM) and small angle x-ray scattering (SAXS). The ionic aggregates of Zn-EMAA are spherical, monodisperse and uniformly-distributed in as-extruded pellets and blown films prepared at low and high blow-up ratio. Thus, although the biaxial stresses of film blowing are sufficient to alter the PE superstructure, the ionic aggregates in Zn-EMAA are unaffected. In contrast, the morphology of Na-EMAA as detected by STEM changes from featureless in the as-extruded pellets to a heterogeneous distribution of Na-rich aggregates in the blown films. This transformation in Na-EMAA morphology is consistent with our earlier study of quiescent annealing suggesting that the morphological change is the result of thermal processing rather than the biaxial stresses of film blowing.

Introduction

Polyethylene based ionomers have found application in a wide variety of areas due to their extraordinary impact toughness along with marked chemical and abrasion resistance. Central to the understanding of these properties is the presence, and morphology of ion-rich aggregates which self assemble on nanometer length scales due to electrostatic interactions between ionic functional groups and acid neutralizing counterions. Research in the area of processing-structure-property relationships in ionomers has received considerable attention in the polymer community however despite the numerous studies, a comprehensive description of ionomer behavior has remained elusive.

Poly(ethylene-*ran*-methacrylic acid) (EMAA) copolymers and cation neutralized ionomers are commonly processed into films via film blowing methods. In this process, the molten polymer is extruded through an annular die at high temperature and pressure. The internal air pressure exerts bi-axial stress and stretches the material to create a thin tubular bubble. This bubble is drawn upward and undergoes rapid solidification as it passes a cooling ring. Following crystallization, the bubble is collapsed and rolled into sheets of thin film. Figure 1 shows a small section of blown film and illustrates the machine direction along the z axis. The y direction, perpendicular to the MD, is commonly known as the transverse direction (TD). The x direction represents the film thickness.

The structure of PE blown films has been extensively studied using many experimental techniques.[1-10] Keller and Machin determined that crystallization under bi-axial stress gives rise to a row-nucleated "shish-kebab" superstructure along the MD in

PE blown films.[2] They established that under low stress conditions, the lamellae grow radially outward from the shish-kebab stem and twist around the crystallographic *b* axis of the unit cell, which is oriented along the TD of the film. Under high stress conditions, there is no pronounced lamellar twisting, but the shish-kebabs and the *c* axis of the unit cell remain oriented along the MD. The amount of stress placed on the film is determined in part by the ratio of the bubble diameter to the die diameter, that is, the blow-up ratio (BUR). Recent work by Lee, Register et al. has shown that in ionomer blown films prepared at low BUR, the expected Keller-Machin superstructure associated with high stress crystallization in PE blown films is obtained.[1] At high BUR, this structure is rotated 90° with the *b* axis of the unit cell now oriented along the MD and the "shish-kebab" morphology along the TD. This morphological change correlates with a change in the preferred direction of tear propagation of these materials.

Here, we investigate the effect of crystallization under bi-axial stress on the morphology of ionic aggregates in semi-crystalline Zn- and Na-neutralized EMAA ionomer blown films. The specimens studied are the same as those investigated by Lee and Register. While that study focused on the spatial orientation of the PE superstructure, we employ the techniques of scanning transmission electron microscopy (STEM) and small angle x-ray scattering (SAXS) to explore the effect of film blowing on the nanoscale morphology. The advantages of STEM imaging lie in the ability to assess the size, shape, and spatial distribution of the ionic aggregates directly without the use of morphological models.

Experimental Section

E.I. Dupont de Nemours provided as-extruded pellets of unneutralized poly(ethylene-*ran*-methacrylic acid) copolymer containing 4.3 mol% acid (EMAA), 46% Zn melt neutralized EMAA with 4.3 mol% acid (Zn-EMAA), and 37% Na melt neutralized EMAA with 4 mol% acid (Na-EMAA). Each of these materials was processed via film blowing using a 3.8 cm extruder operated at 35 rpm, with an extrusion rate of 4.2 kg/h. Extrusion through a 5 cm die was performed at melt temperatures between 205 - 210°C. Blow-up ratio (BUR) ranged from 1.5 to 3.5 and the frost line height was approximately 15 cm. For convenience, these blown films will be designated by the material label followed by the BUR: EMAA 1.5, EMAA 3.5, Zn-EMAA 1.5, Zn-EMAA 3.5, Na-EMAA 1.5, Na-EMAA 3.4.

Upon receipt, the thermal properties of all blown films were characterized by dynamic mechanical analysis (DMA) and differential scanning calorimetry (DSC). DMA was performed with a Rheometrics Solids Analyzer (RSAII) at a frequency of 1 rad/s and a strain amplitude of 4%. A static load of 5 gmf was applied to prevent sample buckling. Temperature was increased stepwise in 5° intervals and held for 5 min prior to each measurement. DSC experiments were performed using a Perkin Elmer DSC operated at a heating rate of 5° C /min.

Two thermal transitions were observed via DMA between -50 C and 100 C for all the blown films studied regardless of neutralization, BUR, or choice of counterion. For both EMAA 1.5 and EMAA 3.5 blown films, a factor of 10 decrease in the dynamic storage modulus was observed at ~5 °C. In addition, a melting transition was observed at ~ 60 °C. Zn- and Na-EMAA blown films processed at both low and high BUR show an

order of magnitude decrease in E′ at ~40 °C and a melting transition at ~70 °C. As expected, partial neutralization with either Zn or Na counterions, increases the first onset thermal transition by ~35°C, while the melting transition is comparable to the unneutralized EMAA films. The thermal transitions evident in the temperature dependence of E′ are also observed via DSC. In addition, the crystallinity for EMAA 1.5, EMAA 3.5, Na-EMAA 1.5 and Na-EMAA 3.4 is ~ 35% while the Zn-EMAA 1.5 and Zn-EMAA 3.5 blown films are somewhat less crystalline at ~25%.

STEM experiments were performed on a JEOL 2010F field emission electron microscope operated at 197kV with a 70μm condenser aperture. Specimen with nominal section thickness of ~50 nm were prepared by cryo-ultramicrotomy at -120°C using a dry diamond knife. STEM images were collected with both high angle annular dark field (HAADF) and bright field (BF) scintillating detectors. Image analysis was performed with Adobe Photoshop 5.0 along with the standard techniques of image enhancement including gray level adjustment and brightness/contrast enhancement. The diameter of a single feature was determined by measuring the number of pixels in line segments at 0°, 45°, 90°, and 135° relative to the horizontal, and computing the mean. The average diameter of many features was calculated as the mean of the diameters for the individual aggregates. Measurements were performed on multiple images at magnification ranging between 500,000x and 800,000x.

X-ray scattering data over a q range between ~1 and 15 nm^{-1} were acquired in our multiple angle x-ray scattering (MAXS) facility, which consists of a Nonius FR591 rotating anode x-ray generator operated at 40kV, 85 mA and a Bruker HiSTAR multiwire detector. The 60 μm-thick films were stacked to a total thickness of ~1mm. The sample

to detector distance was 12 cm and the data were acquired over a 1 hour interval. Two dimensional patterns were integrated azimuthally over 180° to yield intensity vs. q plots.

Results and Discussion

The blown film, Zn-EMAA 1.5, exhibits anisotropic scattering at q ~ 14 nm^{-1} that is representative of a shish-kebab morphology along the MD. This is consistent with the Keller-Machin structure associated with the crystallization of PE blown films under high stress. At higher BUR, Zn-EMAA 3.5, the scattering pattern is rotated by 90° indicating that the shish-kebab morphology is now oriented along the TD. This structural flip was also observed in both unneutralized EMAA (EMAA 1.5, EMAA 3.5) and Na-neutralized (Na-EMAA 1.5, Na-EMAA 3.4) blown films. In contrast, the as-extruded Zn- and Na-EMAA pellets exhibit isotropic crystalline orientation, as expected. These findings are consistent with those of Register et al.[1] An isotropic scattering peak was observed at ~ 3 nm^{-1} for all of the ionomer blown films and as-extruded pellets. This peak, which is traditionally assigned to interparticle interference between spherical ionic aggregates arranged with liquid-like order, was not observed in unneutralized EMAA. The ionomer peak exhibits constant peak intensity (to within ~ 5 %) at all azimuthal angles suggesting an isotropic collection of ionic aggregates in the as-extruded ionomers and the blown films independent of the PE crystalline orientation.

Figure 2 depicts bright field (BF) and high angle annular dark field (HAADF) STEM images of the nanoscale morphology of Zn-EMAA 3.5 blown film. The images of the blown film correspond to the *xy* plane as defined in Figure 1a, the plane perpendicular to the MD; these materials were also imaged in the *xz* plane. In BF STEM, in which the detector is positioned directly below the specimen, the dark features correspond to regions of higher average atomic number (Z) from which the electrons are elastically scattered to high angles. In HAADF STEM, these scattered electrons are detected and

the regions of higher average Z from which they were scattered appear bright. Thus, the features depicted in figure two are 2D projections of 3D nanometer scale Zn-rich aggregates in the presence of a low atomic number carbon-rich matrix.

The STEM images in Figure 3a and 3b depict similar morphologies of Zn-EMAA ionomers in both the as-extruded pellet and blown thin film with BUR = 3.5. Table 1 details the mean diameters of the ionic aggregates in Zn-EMAA ionomer blown films as a function of the BUR and imaging plane (xy and xz). For comparison, the ionic aggregates in as-extruded Zn-EMAA pellets have average diameters of 3.9 $\pm$ 0.7 nm as measured by STEM. In both the pellet and the blown films, the ionic aggregates are spherical in shape and distributed randomly throughout the specimen. In both the *xy* and *xz* imaging planes, the ionic aggregates in the blown films do not appear distorted in shape or size. The number density of the aggregates is independent of the BUR. From the STEM data, we conclude that the film blowing process does not alter the morphology of the ionic aggregates relative to the as-extruded pellets even at high BUR when the crystalline morphology flips.

Figure 3c depicts normalized X-ray intensity vs. q plots for as-extruded Zn-EMAA pellets, Zn-EMAA blown films, and unneutralized EMAA blown film, in the q range from 1 to 8 nm^{-1}. The data show no significant deviation in scattering as a result of film blowing or BUR. This scattering data suggests no change in the size, shape, or spatial distribution of the ionic aggregates in Zn-EMAA due to film blowing, as was observed directly by STEM. This result is similar to that observed by Laurer et al., who report no significant change in the ionic aggregate morphology of Zn-EMAA (4% acid)

ionomers of various neutralization levels between the as-extruded and quiescently annealed ionomers.[11,12]

As-extruded Na-EMAA pellets were imaged and determined to be featureless to within the STEM detection limit of ~ 1 nm. There were no regions of increased average atomic number present in any of these specimens. The STEM images in Figure 4a and 4b represent the morphological variety observed in a single Na-EMAA blown film imaged in the xz plane. Figure 4a depicts a featureless region, while Figure 4b depicts a region containing Na-rich regions with sizes ranging between 25-100 nm. We have also observed well defined boundaries between these two vastly distinct morphological regions and estimate the size of these regions to be on the order of microns. This heterogeneous morphology is present in all STEM images of Na blown films regardless of the imaging plane or BUR. These results on Na-EMAA ionomers are qualitatively similar to those obtained by Taubert et al. who determined that isothermal recrystallization also induces a heterogeneous morphology.[13] Using STEM, Taubert found that the as-extruded Na-EMAA (5% acid, 83% neutralized) material is featureless. After melting (130 °C for 90 minutes), recrystallizing (60 °C for 270 minutes) and quenching, STEM revealed 3 distinct coexisting morphologies: featureless, small (2-15 nm) spherical aggregates, and large (20-160 nm) spherical aggregates. Thus as-extruded Na-EMAA pellets have been observed by STEM to transform from a featureless state, within the limits of STEM detection, to a state of heterogeneous Na distribution during quiescent thermal processing or film blowing. This heterogeneity may be a result of non-uniform mixing during melt neutralization or due to excess Na-containing neutralizing agent.

Figure 4c presents the x-ray scattering data for the Na-neutralized EMAA ionomers. Despite the drastically different morphologies detected by STEM, the SAXS patterns are identical for the as-extruded pellet and the blown films of Na-EMAA. The data does not indicate any change in the breadth or position of the isotropic peak present at ~ 3 nm^{-1} as a function of processing. Evidently, further investigation into the relationship between STEM and SAXS data from ionomers is necessary to resolve these discrepancies such that these techniques may be used in a complementary manner to explore the nanoscale morphology of ionomers.

Conclusion

The crystalline morphology of EMAA ionomers changes with processing, while the percent crystallinity is constant. Specifically, melt extrusion of pellets produces isotropic crystallinity, film blowing at low BUR produces shish kebabs along the machine direction, and film blowing at high BUR produces shish kebabs along the transverse direction. These processing methods and the corresponding changes in crystalline morphology do not alter the morphology of the ionic aggregates in the Zn-EMAA ionomer. As imaged by STEM, the spherical Zn-rich aggregates exhibit the same shape, size and number density for all three processing routes. In contrast, the Na-EMAA ionomer transforms from a featureless morphology (corresponding to the apparent absence of ionic aggregates) produced by melt extrusion to a state of heterogeneous aggregation produced by film blowing according to STEM. As published earlier in a quiescent annealing study, the micron-scale heterogeneity in Na-EMAA ionomers suggests an inhomogeneous Na distribution within the material that is not evident using SAXS, but is inescapable using STEM.

Acknowledgements

Funding was provided by the National Science Foundation (DMR02 - 35106). We acknowledge Dr. David M. Dean (Dupont) and Prof. Richard A. Register (Princeton University) for providing the materials, Lindsey Karpowich for performing dynamic mechanical analysis, Dr. Andreas H. Taubert and Dr. Brian P. Kirkmeyer for helpful discussions and technical assistance with the JEOL 2010F. Nicholas M. Benetatos acknowledges funding provided through an Augustus T. Ashton fellowship at the University of Pennsylvania.

References

(1) Lee, L. W.; Register, R. A.; Dean, D. M. *Journal of Polymer Science: Part B: Polymer Physics* **2005**, *43*, 97-106.

(2) Keller, A.; Machin, M. *J. Macromol. Sci. - Phys* **1967**, *B1*, 41.

(3) Prasad, A.; Shroff, R.; Rane, S.; Beaucage, G. *Polymer* **2001**, *42*, 3103-3113.

(4) Krishnaswamy, R. K. *Journal of Polymer Science: Part B: Polymer Physics* **2000**, *38*, 182-193.

(5) Krishnaswamy, R. K.; Sukhadia, A. M. *Polymer* **2000**, *41*, 9205-9217.

(6) Lu, J.; Sue, H.-J. *Macromolecules* **2001**, *34*, 2015-2017.

(7) Lu, J.; Sue, H.-J.; Rieker, T. P. *Journal of Materials Science* **2000**, *35*, 5169-5178.

(8) Lu, J.; Sue, H.-J.; Rieker, T. P. *Polymer* **2001**, *42*, 4635-4646.

(9) Shanks, R. A.; Drummond, K. M.; Cser, F. *Journal of Polymer Science: Part B: Polymer Physics* **2002**, *83*, 777-784.

(10) Seguela, R.; David, L.; Guichon, O.; Vigier, G. *Journal of Polymer Science: Part B: Polymer Physics* **2003**, *41*, 327-340.

(11) Laurer, J.; Winey, K. I. *Macromolecules* **1998**, *31*, 9106-9108.

(12) Laurer, J.; Winey, K. I.; Kirkemeyer, B. P. *Macromolecules* **2000**, *33*, 507-513.

(13) Taubert, A.; Winey, K. I. *Macromolecules* **2002**, *35*, 7419-7426.

Table

Table 1: Mean diameters, D, and standard deviations of ionic aggregates in Zn-EMAA (12% acid, 46% neutralized) ionomers as a function of the BUR as measured by STEM. Plane coordinates (xy and xz) correspond to imaging directions parallel and perpendicular to the machine direction, respectively.

	D (nm) *xy* plane	D (nm) *xz* plane	D (nm) *xy* and *xz* plane
Zn-EMAA 1.5	3.9 ± 0.7	3.5 ± 0.5	3.7 ± 0.6
Zn-EMAA 3.5	3.9 ± 0.7	3.8 ± 0.7	3.9 ± 0.7

Figure Captions

Figure 1: Schematic defining a coordinate system in blown films with respect to the machine direction (MD). Note the *y* direction is the transverse direction (TD) and the film thickness *x* is significantly thinner than *y* and *z*.

Figure 2: BF and HAADF STEM images of Zn-EMAA 3.5 blown film in the plane perpendicular to the MD. Contrast reversal between BF (top) and HAADF (bottom) images confirms the presence of Zn-rich (higher Z) aggregates amidst a C-rich matrix (lower Z).

Figure 3: Bright field STEM images of Zn-EMAA (12% acid, 46% neutralized) illustrate the similarity between the ionic aggregate morphology of (A) the as-extruded pellets and (B) the blown film as images in the *xy* plane. (C) X-ray scattering data for as-extruded Zn-EMAA pellets and three blown films. The normalized scattering data has been shifted vertically by 100 arbitrary units.

Figure 4: BF STEM images of a Na-EMAA (11% acid, 37% neutralized) ionomer blown film imaged in the *xz* plane show two distinct morphologies: (A) featureless and (B) Na-rich aggregates. (C) X-ray scattering data for as-extruded Na-EMAA pellets and three blown films.

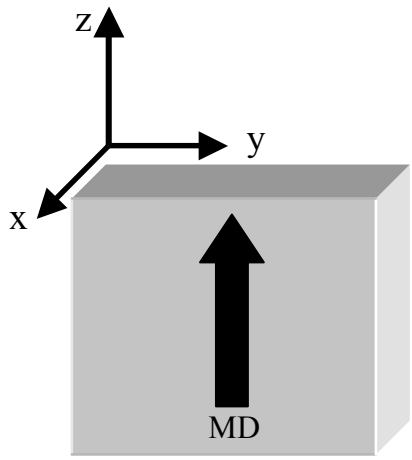

Figure 1

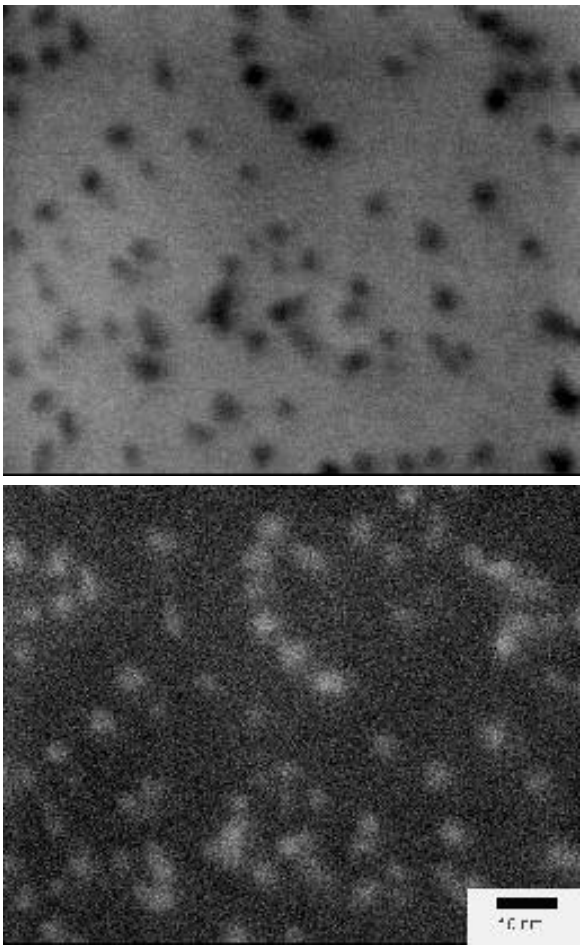

Figure 2

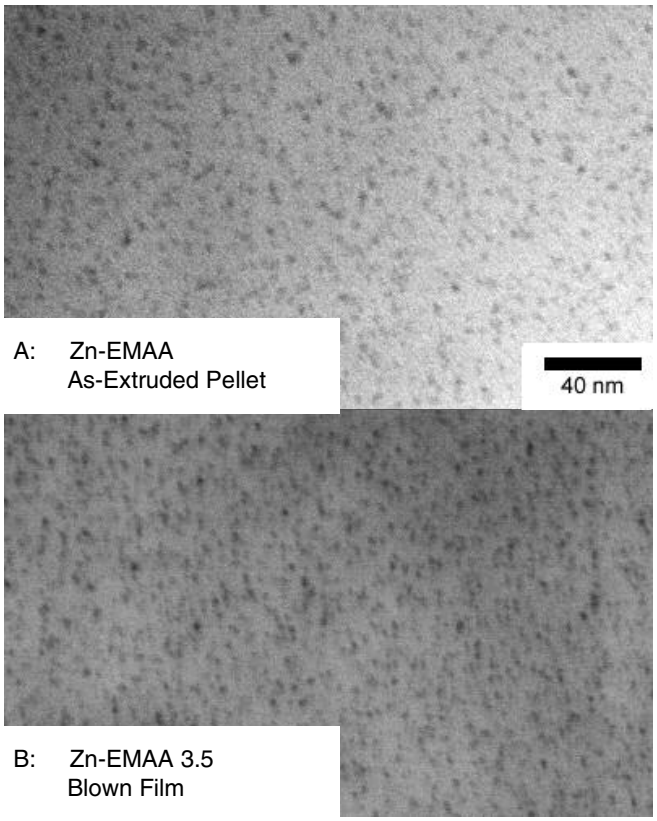
A: Zn-EMAA
As-Extruded Pellet
40 nm
B: Zn-EMAA 3.5
Blown Film

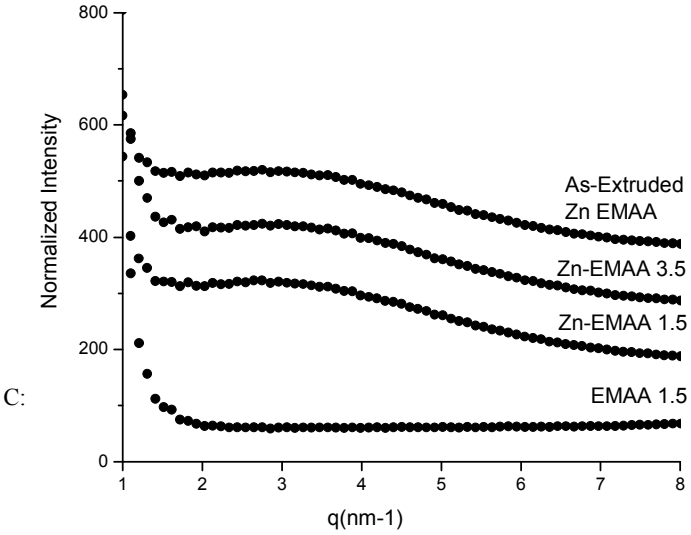
C:
Normalized Intensity
800
600
400
200
0
1
2
3
4
5
6
7
8
q(nm-1)
As-Extruded
Zn EMAA
Zn-EMAA 3.5
Zn-EMAA 1.5
EMAA 1.5

Figure 3

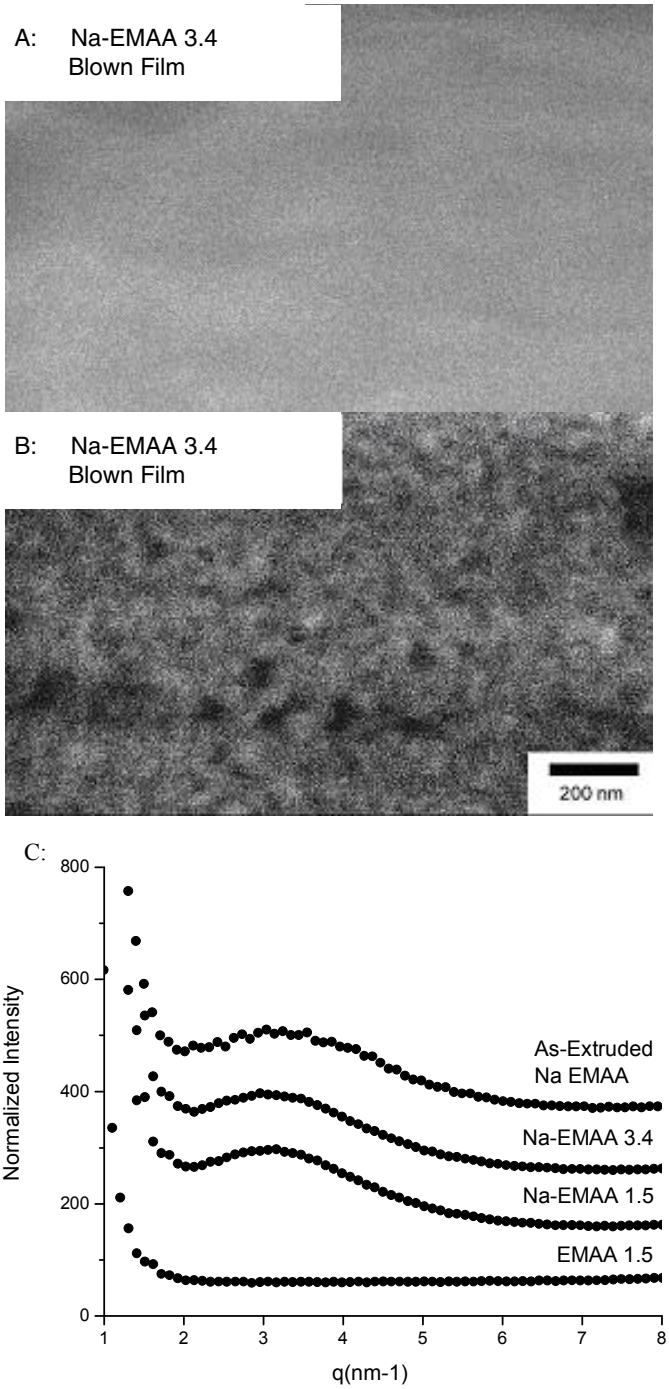
A: Na-EMAA 3.4
Blown Film
B: Na-EMAA 3.4
Blown Film
200 nm
C:
Normalized Intensity
q(nm-1)
As-Extruded
Na EMAA
Na-EMAA 3.4
Na-EMAA 1.5
EMAA 1.5
0
200
400
600
800
1
2
3
4
5
6
7
8

Figure 4